

New isomeric transition in ^{36}Mg : Bridging the N=20 and N=28 islands of inversion

M. Madurga¹, J.M. Christie¹, Z. Xu¹, R. Grzywacz^{1,2}, A. Poves³, T. King¹, J.M. Allmond², A. Chester⁴, I. Cox¹, J. Farr¹, I. Fletcher¹, J. Heideman¹, D. Hoskins¹, A. Laminack², S. Liddick^{4,5}, S. Neupane¹, A.L. Richard^{4,*}, N. Shimizu⁶, P. Shuai^{1,2,†}, K.L. Siegl¹, Y. Utsuno^{7,8}, P. Wagenknecht¹, and R. Yokoyama¹

¹*Dept. of Physics and Astronomy, University of Tennessee, Knoxville, Tennessee 37996, USA*

²*Physics Division, Oak Ridge National Laboratory, Oak Ridge, Tennessee 37830, USA*

³*Departamento de Física Teórica, and IFT UAM-CSIC, Universidad Autónoma de Madrid, 28049, Madrid, Spain*

⁴*National Superconducting Cyclotron Laboratory, Michigan State University, East Lansing, Michigan 48824, USA*

⁵*Department of Chemistry, Michigan State University, East Lansing, Michigan 48824, USA*

⁶*Center for Computational Sciences, University of Tsukuba, 1-1-1, Tennodai Tsukuba, Ibaraki 305-8577, Japan*

⁷*Advanced Science Research Center, Japan Atomic Energy Agency, Tokai, Ibaraki 319-1195, Japan*

⁸*Center for Nuclear Study, University of Tokyo, Hongo, Bunkyo-ku, Tokyo 113-0033, Japan*

(Dated: April 18, 2023)

We observed a new isomeric gamma transition at 168 keV in ^{36}Mg , with a half-life of $T_{1/2}=[130-500](\pm 40)(^{+800}_{-20})_{sys}$ ns. We propose that the observed transition de-excites a new 0^+ isomeric state at 833 keV and populates the previously known first 2^+ state. The existence of this isomer is consistent with the predictions of the large-scale shell model calculations of ^{36}Mg using the *sdpf-u-mix* interaction. The observed excitation energy of the second 0^+ state is caused by the small energy separation between two prolate-deformed configurations where the intruder configuration corresponds to two neutron excitations from the *sd* to the *pf* shell. Within this interpretation, ^{36}Mg becomes the crossing point between nuclei in which ground state deformed/superdeformed configurations are caused by the dominance of N=20 intruders ($^{32,34}\text{Mg}$) and nuclei where deformed configurations are associated with N=28 intruders (^{38}Mg and beyond). We found the lack of three-body monopole corrections in other effective interactions results in a predominance of N=20 intruder configurations past ^{38}Mg incompatible with our observation. We conclude that ^{36}Mg bridges the N=20 and N=28 islands of inversion, forming the so-called Big Island of Deformation.

The large shell gaps in nuclei with "magic" numbers for protons and neutrons emerge from the collective action of the strong forces mediated through pion exchange. However, most nuclei are non-magic, and many are deformed due to the effects of nucleon-nucleon correlations. The surprising emergence of the so-called islands of inversion, where the nuclei with magic numbers are known to be deformed, was attributed to the dominating character of correlations, which the large shell gaps could not suppress. The Island of Inversion centered around magnesium isotopes with neutron "magic" number N=20 has attracted considerable interest [1–5] since its discovery [6]. Negative-parity intruder states ascribed to excitations involving multiple particle-hole configurations between *sd* to the *pf* orbitals indicate a sudden quenching of the N=20 shell closure. Nuclei inside the Island of Inversion are defined by having ground states dominated by such configurations [7]. Further, recent experimental [8] and theoretical [5] studies suggest that particle-hole configurations dominate ground states in this region of the chart of nuclei between the N=20 and the N=28 "magic" numbers. This

forms a so-called Big Island of Deformation, where both neutron "magic" numbers N=20 and N=28 disappear in the magnesium isotopic chain. The quenching of the N=20 and N=28 shell closures is driven by the diminishing effect of the isospin T=0 component of the tensor force as the proton-neutron ratio becomes more asymmetric [9]. Recently developed interactions in the proton/neutron *sd-pf* valence space have had considerable success in reproducing the observed intruder and ground-state configurations of known Island of Inversion nuclei. Some examples are effective interactions such as *sdpf-m* [10], *sdpf-u-mix* [5], or the new interaction *EEdf1*, developed from the chiral expansion at N3LO. [11]. As we shall see later the explicit three body global monopole term proposed with *sdpf-u-mix* is crucial to produce the evolution of the N=20 neutron closure towards N=28 consistent with our observation. Interestingly, each interaction predicts differing microscopic interpretations of the N=20 and N=28 islands of inversion. In all interactions but *sdpf-u-mix*, excited states crossing the N=20 shell closure are substantial in both islands of inversion. On the other hand, *sdpf-u-mix* predicts the N=20 shell closure is restored at ^{40}Mg , postulating instead that deformation is driven exclusively by the breakdown of the N=28 subshell closure. There is currently no experimental data that can resolve these differing interpretations. Delineation of the boundaries of the islands of inversion towards the neutron drip-line is therefore essential to determine

* Current address: Lawrence Livermore National Laboratory, Livermore, CA 94550.

† Current address: Institute of Modern Physics, Chinese Academy of Sciences, Lanzhou, Gansu 730000, China

the disappearance and appearance of the $N=20$ and $N=28$ shell closures respectively [12]. Isomers, long lived excited states, offer an observable with which to track evolving nuclear properties as we study nuclei between shell closures. The half-life of an isomeric state is fully determined by the transition's energy and its electromagnetic transition probability, in turn defined by the wave-functions of the involved states. One such example are the so-called shape isomers, excited states arising from nuclear configurations of different shapes. Low energy excited 0^+ states corresponding to prolate(oblate) deformed configurations [13] may become isomeric when decaying to the first excited 2^+ state corresponding to the ground state band of different deformation.

As of the beginning of 2023, there is only one isomer confirmed and published in either neon or magnesium isotopes, the 0_2^+ state in ^{32}Mg that decays to the 2_1^+ via a 172 keV transition with $T_{1/2} > 10$ ns [14, 15]. Shell model calculations using the *sdpf-u-mix* interaction [16] produce a ground state that is a mixture of deformed (2p-2h) and superdeformed (4p-4h) configurations and an isomeric 0^+ state which is dominated by superdeformed and spherical (0p-0h) components [5]. Notice that *sdpf-u-mix* is the only interaction that locates the isomer close to its experimental excitation energy. In the same calculation, heavier magnesium isotopes were expected to strongly favor quadrupole components before transitioning to the $N=28$ Island of Inversion at ^{40}Mg . This hypothesis is supported by the systematics of the first 2^+ states in $^{34,36,38}\text{Mg}$ [8, 17–19] comparing well with calculations [20].

In this Letter we present the observation of a new isomeric gamma transition at 168 keV in ^{36}Mg , assigned to a second 0^+ state feeding the first 2^+ state. The analysis of the time structure of 168 keV gamma-ray events following the ion implantation results in a half-life of $T_{1/2} = [130-500](\pm 40)_{\text{tran}}({}^{+800}_{-20})_{\text{sys}}$ ns. We present an interpretation of the nature of the new second 0^+ state and the evolution of intruder configurations in the magnesium isotopic chain from $N=20$ to $N=28$ using shell model calculations with the *sdpf-u-mix* interaction [5]. Our calculations indicate the isomer naturally arises from gradually restoring the $N=20$ shell closure as the neutron $0f_{7/2}$ orbital is occupied towards the $N=28$ subshell closure.

Experiment. The experiment was performed at the National Superconducting Cyclotron Laboratory (NSCL) at Michigan State University. A ^{48}Ca beam, 80 pA average intensity at 140 MeV/u, was fragmented in a 846 mg/cm² thick Be target at the entrance of the fragment separator, A1900 [21], to produce the nuclei of interest, a "cocktail" beam consisting of isotopes from boron ($Z=5$) to aluminum ($Z=13$). In order to identify the different species, we measured the ion's time-of-flight between a scintillator located in the focal plane of A1900 and a Silicon detector (Si PIN) placed in front of our experimental setup. Combining with the energy loss in the Si PIN allowed us to perform particle identification (PID) in the beam, as shown in Fig. 1.

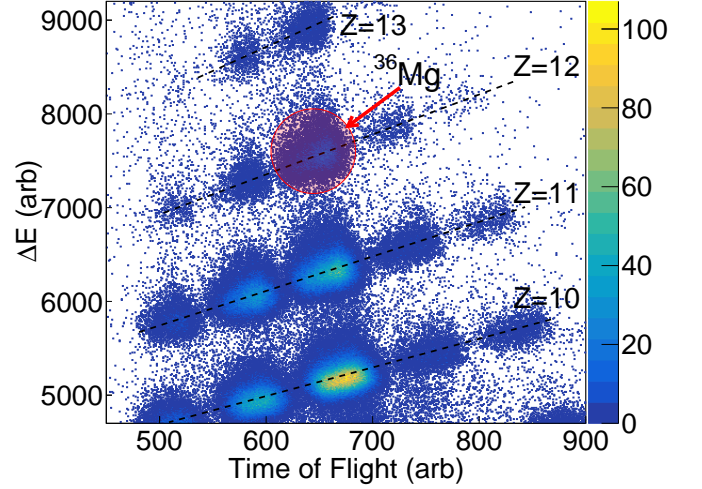


FIG. 1. Two dimensional energy loss (ΔE) v. time of flight particle identification plot for all ion implants between $Z=10$ (bottom row) and $Z=13$ (top row). Magnesium-36 is highlighted by the red circle. We also searched for isomers in $^{25-29}\text{F}$ isotopes (not shown).

We implanted the "cocktail" beam in a 12-mm thick YSO detector (Yttrium Orthosilicate, Y_2SiO_5) [22] allowing for recording energies and timestamps of ion implantation and beta-decay events. The YSO detector was surrounded on one side by 48 VANDLE modules [23] providing a total neutron detection efficiency of 11% at 1 MeV. On the other side of the setup, three HPGe clovers from the CLARION array [24] resulting in gamma detection of 1.3% efficiency at 1 MeV.

We searched for isomers in all Fluorine, Neon, Sodium, Magnesium, and Aluminum isotopes shown in Fig. 1 by analyzing the gamma rays emitted between 40 ns and 500 ns after ion implantation, correlated to each individual isotope using the PID plot (Fig. 1). We excluded the first 40 ns in order to remove the Gaussian tail of the prompt implantation "flash". We did not identify isomeric transitions in any F, Ne, Na, Mg, or Al isotope except for ^{36}Mg . In ^{36}Mg , we observe a prominent gamma transition at 168 keV, see Fig. 2. The top right panel of Fig. 2 shows the gamma spectrum between 500 and 750 keV. We marked several gamma lines corresponding to germanium (\dagger) and iron (\S) neutron inelastic scattering [25], as well as the 511 keV line corresponding to positron annihilation ($\#$). Imposing total event multiplicity one, we expect close to no background in the 600 to 700 keV region. Therefore, we identified the 3(2) counts at 665 keV to the de-excitation of the first excited state in ^{36}Mg [8, 17, 18, 26–28]. The first excited state spin and parity was confirmed to be 2^+ by the recent measurement of the quadrupole electromagnetic transition strength [18]. Since the 2^+ state in ^{36}Mg was not observed to be isomeric, we propose the isomeric state in ^{36}Mg decays to the 2^+ state via emitting the 168 keV

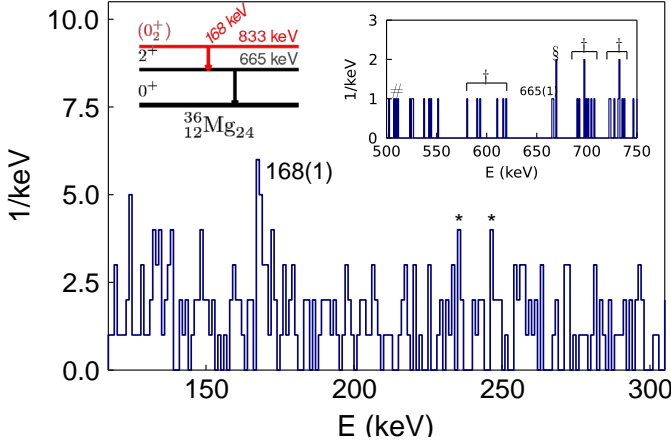


FIG. 2. Delayed gamma energy spectrum in coincidence with ^{36}Mg implantation events. The most prominent line corresponds to the new isomeric transition at 168 keV ([*] marks background lines). The top left panel shows the ^{36}Mg partial level scheme. The top right panel shows the gamma spectrum between 500 and 750 keV, including the ^{36}Mg 665 keV transition and other background lines (see text for details).

gamma ray. We calculated the number of counts we would observe if the new 168 keV line and the 665 keV line form a gamma cascade. We observe 5(4) counts in the 168 keV peak above background. Using efficiencies of 1.8% at 168 keV and 1.5% at 665 keV we expect 4(3) counts at 665 keV, compatible with the observed 3(2) counts. Considering the placement of the other known isomer in neutron rich magnesium isotopes (^{32}Mg), the most likely explanation places the new 168 keV isomer as the de-excitation of a new 833 keV 0^+ state directly to the known 665 2_1^+ state in ^{36}Mg (top left inset in Fig. 2).

We performed a log likelihood analysis of the gamma activity after ion implantation, see Fig. 3. The left panel shows the time distribution of gamma events after ion implantation for the photopeak gate (167 to 169 keV). The right panel shows the time distribution of background events ($166 < E_\gamma < 167$ keV and $169 < E_\gamma < 170$ keV). First, in order to estimate the component arising from the tail of the Gaussian distribution of the ion implantation Bremsstrahlung flash, we fitted the time distribution of the background gate to an exponential function (Fig. 3b). Then, we constructed a double exponential distribution, corresponding to photopeak and background combined, 50% each as per the gamma energy spectrum estimate. We fitted the photopeak gate, obtaining $T_{1/2} = 90^{(+410)}_{(-50)}$ ns. We also studied the systematic uncertainty due to the shape of the tail of the implantation flash. In order to progressively remove the background tail, we performed fits to samples starting at increasingly later times, between 50 ns to 100 ns. Finally, we calculated the shortest observable half-life considering the transit time (500 ns) in A1900, and assuming

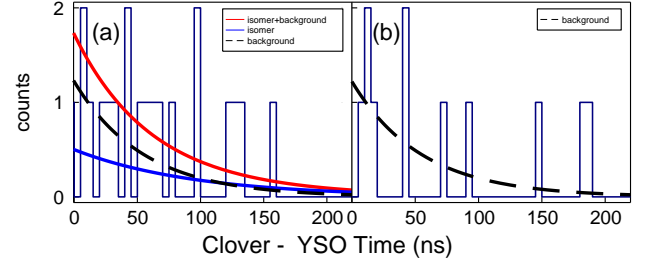


FIG. 3. (Left) Time distribution of gamma activity after ion implantation gated on the 168 keV photopeak with background (black-dashed, see right panel), isomer (blue) and combined (red) fits overlaid. (Right) Distribution of gamma events gated on the Compton background surrounding the photopeak.

an isomer population of 10% in the fragmentation reaction producing ^{36}Mg , obtaining 130(40) ns. Given the statistical constraints due to the size of our sample, the limits imposed by the transit time in A1900, and the systematic effects mentioned above, we provide a half-life range for the 168 keV isomer, at 3σ confidence level, of $T_{1/2} = [130-500](\pm 40)_{\text{tran}}^{(+800)}_{(-20)} \text{ ns}$. The resulting half-life range corresponds to $B(E2) = [12-50]^{(+30)}_{(-1)} \text{ tran}^{(+10)}_{(-7)} \text{ sys e}^2 \text{ fm}^4$.

Discussion. In the heavy Magnesium isotopes two neutron shell closures are washed out by the presence of intruder configurations whose energy, fostered by the quadrupole correlations, make them dominant in the ground states, giving rise to the N=20 and N=28 Islands of Inversion. As explained in ref. [5] we submit that the effective interaction for this wide region should include a three body monopole correction of the form:

$$\delta V_{pf} = \frac{1}{2} n_{pf} \left(\frac{18}{A} \right)^{1/3} 75 \text{ keV} \quad (1)$$

which restores the N=20 closure in ^{40}Mg as it is required by consistency and naturalness of the very shell model with configuration interaction (SM-CI) approach (n_{pf} is the number of neutrons in the pf shell in the normal filling approximation). Notice however that in ref. [29] the *EEdf1* interaction produces a completely different picture because the neutron $0d_{3/2}$ orbit is only half filled already in ^{30}Mg and remains so even in the ^{40}Mg ground state.

We proceed now to explain the results of our SM-CI calculations using the *sdpf-u-mix* interaction [5]. The calculations are performed with the code Antoine [30]. It is interesting to follow the location of the intruder configurations before mixing as the number of neutrons increase. We denote by $0\hbar\omega$ the normal filling configuration, and by $x\hbar\omega$, with $x = 0, 2, 4$ etc, the xp - xh neutron excitations across N=20. Their relative position gives us a clear hint of what will be the structure of the low lying states after full diagonalization, although the details of the spectroscopy depend on many other ingredients, in particular on the off-diagonal

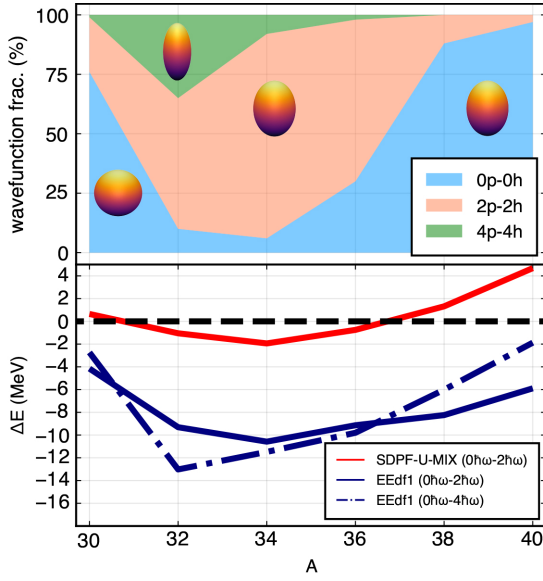


FIG. 4. (Bottom panel) Energy splitting between the normal filling configuration and the intruder state corresponding to the promotion of two neutrons across the $N=20$ magic shell closure ($2\hbar\omega$), in the heavy Magnesium isotopes, calculated with *sdpf-u-mix* (red) and *EEdf1* (blue corresponds to $2\hbar\omega$ and dash-dotted blue to 4 neutron excitations $4\hbar\omega$). (Upper panel) Percentage of np-nh configurations in the theoretical wave functions of the ground states of the Magnesium isotopes, 0p-0h (blue), 2p-2h (orange), 4p-4h (green), using the *sdpf-u-mix* interaction. The cartoon nuclei represent the shape of each configuration.

matrix elements between the states calculated at fixed values of $x\hbar\omega$ differing in two units. As a first step, we study the relative location of the 0^+ band heads of the $0\hbar\omega$ and $2\hbar\omega$ configurations. The results are shown in the bottom panel of Fig. 4. It is seen that the intruder states cease to be clearly dominant at $A=36$. The increase of the quadrupole moment Q_{spec} of the 6p-2h configuration with respect to the 4p-0h one is small, therefore the gain in quadrupole correlation energy of the latter barely compensates its loss of monopole energy. As a consequence, the 6p-2h configuration in ^{36}Mg is not as dominant as the 4p-2h one in ^{34}Mg . Beyond $A=36$ ($N=24$), the 6p-0h and 8p-0h configurations are re-established as the main components in the ground states of ^{38}Mg and ^{40}Mg . This is in stark contrast with the calculation using the *EEdf1* interaction shown in the bottom panel of Fig. 4. Here, intruder configurations, both $2\hbar\omega$ and $4\hbar\omega$ remain dominant across the entire isotopic chain, precluding mixing with $0\hbar\omega$ normal-filling configurations. However, we must point out, as seen in Fig. 4, the energies of the $2\hbar\omega$ and $4\hbar\omega$ configurations are quasi-degenerate for ^{34}Mg and ^{36}Mg . As we will see later, large off-diagonal elements in *EEdf1* result in a strong repulsive force when considering two-state mixing, resulting in high energy 0_2^+ states except for the postulated second 0^+ in ^{40}Mg [29].

It is precisely the crossing of the 4p-0h and 6p-2h configurations in ^{36}Mg what might explain the very low energy of the excited 0^+ . In the full calculation, *sdpf-u-mix* places the excited 0^+ in ^{36}Mg at 1.55 MeV, and produces a ^{36}Mg which is non axially-symmetric (triaxial) with low energy excitations (gamma band). These low energy states are not compatible with the existence of a 0^+ isomer as seen in the present experiment. Given that the amplitude of the 8p-4h configurations is negligible, the problem can be translated into a two state model including only the 4p-0h and the 6p-2h states discussed above. According to the calculated Q_{spec} moments within the bands both are prolate deformed. If the energies of the 4p-0h and 6p-2h states were degenerate before mixing (and this is nearly the case), the final splitting of the two 0^+ states would be roughly equal to $2W$, with $W = \langle 4p - 0h(0^+) | V | 6p - 2h(0^+) \rangle$. In fact, $W=730$ keV in ^{36}Mg , and this sets a theoretical lower limit to the excitation energy of the isomer 0^+ , within the two state model. The value in the complete diagonalization is very much in line with this estimate. Thus, the only way to get the splitting right is via a reduction of the value of W , which is dominated by the off-diagonal pairing interaction between the sd and the pf-shell neutron orbits. Hence we are led to make an “ad hoc” 10% reduction of the off diagonal pairing matrix elements for $n_{pf} > 0$, bringing W down to about 500 keV. With this choice, the resulting composition of the ground states of the Magnesium isotopes is as depicted in the upper panel of Figure 4. We see the intruder ($2, 4\hbar\omega$) configurations are dominant in $^{32,34,36}\text{Mg}$, while the normal-filling ($0\hbar\omega$) states take the majority of the wavefunction in $^{30,38,40}\text{Mg}$. This trend is consistent with the restoration of the $N=20$ shell closure as we approach the $N=28$ subshell, disfavoring particle-hole excitations across the $N=20$ shell gap.

The spectroscopic results for ^{36}Mg are gathered in Table I. The excitation energies are in good agreement with the

TABLE I. Theoretical excitation energies (in MeV), Q_{spec} in efm^2 and $B(E2)$'s (in e^2fm^4), for ^{36}Mg , using the *sdpf-u-mix* interaction.

J^π	$E(th)$	Q_{spec}	$J^\pi(f)$	$B(E2)$
0_1^+	0.0			
2_1^+	0.58	-23	0_1^+	130
0_2^+	1.02		2_1^+	5
2_2^+	1.43	-15	0_1^+	2
2_2^+			2_1^+	1
2_2^+			0_2^+	120
4_1^+	1.73	-23	2_1^+	183
4_1^+			2_2^+	1

present experimental result for the 0^+ isomer and with the results of reference [17] for the yrast 2^+ and 4^+ . Using the *EEdf1* interaction in Monte Carlo Shell Model, we obtained a 0_2^+ energy of 2.32 MeV with a $B(E2)$ of $0.4 e^2fm^4$, using effective charges of 1.25 e and 0.25 e for protons and neutrons respectively, not compatible with our obser-

vation. We must stress that the presence of an isomer in ^{36}Mg is important beyond the value of its excitation energy. As mentioned above, our calculations with the *sdpf-u-mix* interaction show different nuclear structure depending on the energy of the 0_2^+ state, from a triaxial solution if it were not isomeric, to a case of two coexisting prolate bands. Figure 4 and the E2 properties listed in table I show the lowest band is dominated by $2\hbar\omega$ configurations and the excited one by $0\hbar\omega$ configurations. A very prominent feature of them is that the configuration mixing between the two bands is almost absent. In particular, the $B(E2)$ from the isomer to the yrast 2^+ is small, compatible with the experimental value extracted from its lifetime. Let's mention finally that the crossover from the dominance of the $0f_{7/2}$ orbit to a massive occupation of the $1p_{3/2}$ orbit, takes place at $N=24$ as well, paving the way to the $N=28$ Island of Inversion.

Conclusions. We observed a new 168 keV isomer in ^{36}Mg , with a half-life of $[130-500](\pm 40)_{\text{tran}}^{(+800)}_{(-20)}_{\text{sys}}$ ns at 3σ confidence level. From the observation of a 665 keV gamma line in the prompt gamma spectrum, we deduce that it corresponds to a new 0^+ state at 833 keV de-exciting to the known 665 keV 2^+ state [18]. To elucidate the microscopic origin of this isomer we performed shell model calculations using the *sdpf-u-mix* interaction. We propose the observed low excitation energy of the state arises from two coexisting prolate deformed configurations consisting of the normal-filling and intruder two-neutron excitations respectively. We predict that, for $N > 20$ Mg isotopes, as the neutron $0f_{7/2}$ orbital is gradually filled, the $N=20$ shell closure is restored while the $N=28$ subshell closure is quenched. Therefore, the quasi-degeneracy between normal and intruder configurations occurs only for ^{36}Mg . In contrast, other effective interactions used so far in the region predict substantial quenching of the $N=20$ shell closure even past ^{38}Mg . We postulate the discrepancy arises from the inclusion, or lack of thereof, of three-body corrections into the monopole part of the effective interaction. The isomer presented in this Letter supports that ^{36}Mg is the bridge between the $N=20$ island of inversion centered around ^{32}Mg and the $N=28$ island of inversion centered in ^{40}Mg . As a direct consequence we anticipate no isomers will be present in $^{34,38}\text{Mg}$. Thanks to the large yields of magnesium isotopes afforded at the recently commissioned FRIB facility in MSU (or RIKEN, Japan), this hypothesis may be tested in the near future.

Acknowledgments. We thank Augusto Macchiavelli for the fruitful discussions during the preparation of this Letter. The isotope(s) used in this research was supplied by the Isotope Program within the Office of Nuclear Physics in the Department of Energy's Office of Science. The Lanczos shell-model calculation using the *EEdf1* interaction was performed with the code KSHELL [31]. This research was sponsored in part by the National Nuclear Security Administration under the Stewardship Science Academic Alliances program through DOE Cooperative

Agreements No. DE-NA0003899 and DE-NA0004068. This research was also sponsored by the Office of Nuclear Physics, U. S. Department of Energy under contract DE-FG02-96ER40983 (UT) and DE-SC0020451 (MSU). This research was sponsored in part by National Science Foundation under the contract NSF-MRI-1919735. This work was also supported by the National Nuclear Security Administration through the Nuclear Science and Security Consortium under Award No. DE-NA0003180 and the Stewardship Science Academic Alliances program through DOE Award No. DOE-DE-NA0003906. N.S. and Y.U. acknowledge computer resources provided by U. Tsukuba MCRP program (woi22i022) and "Program for Promoting Researches on the Supercomputer Fugaku" (JP-MXP1020200105).

A.P. is supported by grants CEX2020-001007-S funded by MCIN/AEI/10.13039/501100011033 and PID2021-127890NB-I00.

-
- [1] A. Poves and J. Retamosa, *Physics Letters B* **184**, 311 (1987).
 - [2] E. K. Warburton, J. A. Becker, and B. A. Brown, *Phys. Rev. C* **41**, 1147 (1990).
 - [3] K. Heyde and J. L. Wood, *Journal of Physics G: Nuclear and Particle Physics* **17**, 135 (1991).
 - [4] N. Fukunishi, T. Otsuka, and T. Sebe, *Physics Letters B* **296**, 279 (1992).
 - [5] E. Caurier, F. Nowacki, and A. Poves, *Physical Review C - Nuclear Physics* **90**, 014302 (2014).
 - [6] C. Thibault, R. Klapisch, C. Rigaud, A. M. Poskanzer, R. Prieels, L. Lessard, and W. Reisdorf, *Phys. Rev. C* **12**, 644 (1975).
 - [7] G. Neyens, M. Kowalska, D. Yordanov, K. Blaum, P. Himpe, P. Lievens, S. Mallion, R. Neugart, N. Vermeulen, Y. Utsuno, and T. Otsuka, *Phys. Rev. Lett.* **94**, 022501 (2005).
 - [8] H. L. Crawford, P. Fallon, A. O. Macchiavelli, P. Doornenbal, N. Aoi, F. Browne, C. M. Campbell, S. Chen, R. M. Clark, M. L. Cortes, M. Cromaz, E. Ideguchi, M. D. Jones, R. Kanungo, M. MacCormick, S. Momiyama, I. Murray, M. Niikura, S. Paschalis, M. Petri, H. Sakurai, M. Salathe, P. Schrock, D. Steppenbeck, S. Takeuchi, Y. K. Tanaka, R. Taniuchi, H. Wang, and K. Wimmer, *Physical Review Letters* **122**, 052501 (2019).
 - [9] T. Otsuka, T. Suzuki, R. Fujimoto, H. Grawe, and Y. Akaishi, *Physical Review Letters* **95**, 232502 (2005).
 - [10] Y. Utsuno, T. Otsuka, T. Mizusaki, and M. Honma, *Phys. Rev. C* **60**, 054315 (1999).
 - [11] N. Tsunoda, T. Otsuka, N. Shimizu, M. Hjorth-Jensen, K. Takayanagi, and T. Suzuki, *Phys. Rev. C* **95**, 021304(R) (2017).
 - [12] K. Fosse, J. Rotureau, N. Michel, and W. Nazarewicz, *Phys. Rev. C* **96**, 024308 (2017).
 - [13] J. H. Hamilton, A. V. Ramayya, W. T. Pinkston, R. M. Ronningen, G. Garcia-Bermudez, H. K. Carter, R. L. Robinson, H. J. Kim, and R. O. Sayer, *Phys. Rev. Lett.* **32**, 239 (1974).

- [14] K. Wimmer, T. Kröll, R. Krücken, V. Bildstein, R. Gernhäuser, B. Bastin, N. Bree, J. Diriken, P. Van Duppen, M. Huyse, N. Patronis, P. Vermaelen, D. Voulot, J. Van de Walle, F. Wenander, L. M. Fraile, R. Chapman, B. Hadinia, R. Orlandi, J. F. Smith, R. Lutter, P. G. Thirolf, M. Labiche, A. Blazhev, M. Kalkühler, P. Reiter, M. Seidlitz, N. Warr, A. O. Macchiavelli, H. B. Jeppesen, E. Fiori, G. Georgiev, G. Schrieder, S. Das Gupta, G. Lo Bianco, S. Nardelli, J. Butterworth, J. Johansen, and K. Riisager, *Phys. Rev. Lett.* **105**, 252501 (2010).
- [15] R. Elder, H. Iwasaki, J. Ash, D. Bazin, P. C. Bender, T. Braunroth, B. A. Brown, C. M. Campbell, H. L. Crawford, B. Elman, A. Gade, M. Grinder, N. Kobayashi, B. Longfellow, A. O. Macchiavelli, T. Mijatović, J. Pereira, A. Revel, D. Rhodes, J. A. Tostevin, and D. Weisshaar, *Phys. Rev. C* **100**, 041301(R) (2019).
- [16] A. Poves, *Journal of Physics G: Nuclear and Particle Physics* **43**, 024010 (2016).
- [17] P. Doornenbal, H. Scheit, S. Takeuchi, N. Aoi, K. Li, M. Matsushita, D. Steppenbeck, H. Wang, H. Baba, H. Crawford, C. R. Hoffman, R. Hughes, E. Ideguchi, N. Kobayashi, Y. Kondo, J. Lee, S. Michimasa, T. Motobayashi, H. Sakurai, M. Takechi, Y. Togano, R. Winkler, and K. Yoneda, *Physical Review Letters* **111**, 212502 (2013).
- [18] P. Doornenbal, H. Scheit, S. Takeuchi, N. Aoi, K. Li, M. Matsushita, D. Steppenbeck, H. Wang, H. Baba, E. Ideguchi, N. Kobayashi, Y. Kondo, J. Lee, S. Michimasa, T. Motobayashi, A. Poves, H. Sakurai, M. Takechi, Y. Togano, and K. Yoneda, *Physical Review C* **93**, 044306 (2016).
- [19] H. L. Crawford, P. Fallon, A. O. Macchiavelli, R. M. Clark, B. A. Brown, J. A. Tostevin, D. Bazin, N. Aoi, P. Doornenbal, M. Matsushita, H. Scheit, D. Steppenbeck, S. Takeuchi, H. Baba, C. M. Campbell, M. Cromaz, E. Ideguchi, N. Kobayashi, Y. Kondo, G. Lee, I. Y. Lee, J. Lee, K. Li, S. Michimasa, T. Motobayashi, T. Nakamura, S. Ota, S. Paschalis, M. Petri, T. Sako, H. Sakurai, S. Shimoura, M. Takechi, Y. Togano, H. Wang, and K. Yoneda, *Phys. Rev. C* **89**, 041303(R) (2014).
- [20] F. Nowacki, A. Obertelli, and A. Poves, *Progress in Particle and Nuclear Physics* **120**, 103866 (2021).
- [21] D. J. Morrissey, B. M. Sherrill, M. Steiner, A. Stolz, and I. Wiedenhoever, *Nuclear Instruments and Methods in Physics Research, Section B: Beam Interactions with Materials and Atoms* **204**, 90 (2003).
- [22] R. Yokoyama, M. Singh, R. Grzywacz, A. Keeler, T. T. King, J. Agramunt, N. T. Brewer, S. Go, J. Heideman, J. Liu, S. Nishimura, P. Parkhurst, V. H. Phong, M. M. Rajabali, B. C. Rasco, K. P. Rykaczewski, D. W. Stracener, J. L. Tain, A. Tolosa-Delgado, K. Vaigneur, and M. Wolińska-Cichocka, *Nuclear Instruments and Methods in Physics Research, Section A: Accelerators, Spectrometers, Detectors and Associated Equipment* **937**, 93 (2019).
- [23] W. A. Peters, S. Ilyushkin, M. Madurga, C. Matei, S. V. Paulauskas, R. K. Grzywacz, D. W. Bardayan, C. R. Brune, J. Allen, J. M. Allen, Z. Bergstrom, J. Blackmon, N. T. Brewer, J. A. Cizewski, P. Copp, M. E. Howard, R. Ikeyama, R. L. Kozub, B. Manning, T. N. Massey, M. Matos, E. Merino, P. D. O'Malley, F. Raiola, C. S. Reingold, F. Sarazin, I. Spassova, S. Taylor, and D. Walter, *Nuclear Instruments and Methods in Physics Research, Section A: Accelerators, Spectrometers, Detectors and Associated Equipment* **836**, 122 (2016).
- [24] C. J. Gross, T. N. Ginter, D. Shapira, W. T. Milner, J. W. McConnell, A. N. James, J. W. Johnson, J. Mas, P. F. Mantica, R. L. Auble, J. J. Das, J. L. Blankenship, J. H. Hamilton, R. L. Robinson, Y. A. Akovali, C. Baktash, J. C. Batchelder, C. R. Bingham, M. J. Brinkman, H. K. Carter, R. A. Cunningham, T. Davinson, J. D. Fox, A. Galindo-Uribarri, R. Grzywacz, J. F. Liang, B. D. Macdonald, J. Mackenzie, S. D. Paul, A. Piechaczek, D. C. Radford, A. V. Ramayya, W. Reviol, D. Rudolph, K. Rykaczewski, K. S. Toth, W. Weintraub, C. Williams, P. J. Woods, C.-H. Yu, and E. F. Zganjar, *Nuclear Instruments and Methods in Physics Research A* **450**, 12 (2000).
- [25] M. Baginova, P. Vojtyla, and P. P. Povinec, *Nuclear Instruments and Methods in Physics Research, Section A: Accelerators, Spectrometers, Detectors and Associated Equipment* **897**, 22 (2018).
- [26] A. Gade, P. Adrich, D. Bazin, M. D. Bowen, B. A. Brown, C. M. Campbell, J. M. Cook, S. Ettenauer, T. Glasmacher, K. W. Kemper, S. McDaniel, A. Obertelli, T. Otsuka, A. Ratkiewicz, K. Siwek, J. R. Terry, J. A. Tostevin, Y. Utsuno, and D. Weisshaar, *Physical Review Letters* **99**, 072502 (2007).
- [27] N. Kobayashi, T. Nakamura, Y. Kondo, J. A. Tostevin, Y. Utsuno, N. Aoi, H. Baba, R. Barthelemy, M. A. Famiano, N. Fukuda, N. Inabe, M. Ishihara, R. Kanungo, S. Kim, T. Kubo, G. S. Lee, H. S. Lee, M. Matsushita, T. Motobayashi, T. Ohnishi, N. A. Orr, H. Otsu, T. Otsuka, T. Sako, H. Sakurai, Y. Satou, T. Sumikama, H. Takeda, S. Takeuchi, R. Tanaka, Y. Togano, and K. Yoneda, *Physical Review Letters* **112**, 242501 (2014).
- [28] S. Michimasa, Y. Yanagisawa, K. Inafuku, N. Aoi, Z. Elekes, Z. Fulop, Y. Ichikawa, N. Iwasa, K. Kurita, M. Kurokawa, T. Machida, T. Motobayashi, T. Nakamura, T. Nakabayashi, M. Notani, H. J. Ong, T. K. Onishi, H. Otsu, H. Sakurai, M. Shinohara, T. Sumikama, S. Takeuchi, K. Tanaka, Y. Togano, K. Yamada, M. Yamaguchi, and K. Yoneda, *Physical Review C* **89**, 054307 (2014).
- [29] N. Tsunoda, T. Otsuka, K. Takayanagi, N. Shimizu, T. Suzuki, Y. Utsuno, S. Yoshida, and H. Ueno, *Nature* **587**, 66 (2020).
- [30] E. Caurier, G. Martínez-Pinedo, F. Nowacki, A. Poves, and A. P. Zuker, (2005).
- [31] N. Shimizu, T. Mizusaki, Y. Utsuno, and Y. Tsunoda, *Computer Physics Communications* **244**, 372 (2019).